

COLLOCATION METHODS BASED ON RADIAL BASIS FUNCTIONS FOR THE COUPLED KLEIN-GORDON-SCHRÖDINGER EQUATIONS*

AHMAD GOLBABAI[†] AND ALI SAFDARI-VAIGHANI[‡]

Abstract. This paper presents radial basis function (RBF) collocation methods for the coupled Klein-Gordon-Schrödinger equations. Unlike traditional mesh oriented methods, RBF collocation methods require only a scattered set of nodes in the domain where the solution is approximated. For the RBF collocation method in finite difference mode (RBF-FD), weights for the finite difference formula are obtained by solving local RBF interpolation problems set up around each node in the computational domain. We show that the RBF-FD method has good accuracy and a sparse coefficient matrix, as compared to the global form of the RBF collocation method and other methods.

Key words. Collocation methods, coupled Klein-Gordon-Schrödinger equations, radial basis functions (RBF).

AMS subject classifications. 65N06, 65N40, 65D25, 35Q51.

1. Introduction. Nonlinear phenomena play a crucial role in a variety of scientific fields, especially in fluid mechanics, solid state physics, particle physics, plasma waves and chemical physics. In this paper, we consider the coupled Klein-Gordon-Schrödinger (KGS) equations

$$(1.1) \quad \begin{aligned} i v_t + v_{xx} + v u &= 0, \\ u_{tt} - u_{xx} + u - |v|^2 &= 0, \end{aligned}$$

with $(x, t) \in \Omega \times (0, T]$ and initial conditions

$$u(x, 0) = u_0(x), \quad u_t(x, 0) = u_{t0}(x), \quad v(x, 0) = v_0(x), \quad x \in \Omega,$$

and zero boundary conditions

$$u(x, t) = v(x, t) = 0, \quad (x, t) \in \partial\Omega \times (0, T],$$

where Ω is a bounded domain in \mathbb{R} and $\partial\Omega$ is the smooth boundary of Ω . The equations (1.1) describe the dynamics of a conserved complex nucleon field v , interacting with a neutral real scalar meson field u . The KGS equations can be considered a generalization of the classical model of Yukawa interaction [8], which goes back to 1935. For more physical details we refer the reader to Yukawa [22].

This problem has been the subject of research for many years and has motivated a series of papers in physics and mathematics. The well-posedness of the Klein-Gordon-Schrödinger equations has been studied by many authors such as Bachelot [1], Hayashi and Von Wahl [12], Fukuda and Tsutsumi [9]. Guo and Miao [11] studied the asymptotic behavior of the solution for these equations. In [19], the authors discussed the initial boundary value problem of Klein-Gordon-Schrödinger equations. Numerical methods such as the homotopy analysis method [14], the conservative spectral method [21], and the Crank-Nicolson method with time-splitting spectral discretization [2] have been used to solve this problem.

In the last decade, collocation methods based on Radial Basis Functions (RBF) became important for obtaining the numerical solution of various ordinary differential equations

*Received February 9, 2011. Accepted January 24, 2012. Published online March 6, 2012. Recommended by Andrew Wathen.

[†]School of Mathematics, Iran University of Science and Technology, Narmak, Tehran, Iran (golbabai@iust.ac.ir).

[‡]Iran University of Science and Technology, Narmak, Tehran, Iran, and Department of Mathematics and Statistics, Allameh Tabatabaie University, Tehran, Iran (a.safdari@iust.ac.ir).

(ODEs) and partial differential equations (PDEs) [4, 7, 10, 16, 20]. These methods are designed to overcome the limitations of methods based on pseudospectral (PS) and mesh-based methods, such as the finite difference method (FDM) and the finite element method (FEM). The RBF-based collocation methods have the advantage of not requiring a mesh, so that the approximate solution is represented entirely in relation to scattered node/data points. Such methods can be easily extended to higher dimensions.

In this work, we investigate accurate methods based on global and local RBF collocation schemes, to study the dynamics of the equations (1.1). In the local form of the RBF collocation schemes, the spatial derivatives for each node can be approximated by local stencils. This allows us to have flexibility in choosing these stencils [18]. The key points in designing our new numerical methods consist of discretizing spatial derivatives by global and local RBF interpolants at scattered points, and solving the resulting system of ordinary differential equations.

The layout of the paper is the following. In Section 2, the properties of RBFs and their application to solving interpolation problems are discussed. Section 3 deals with RBF collocation methods for the KGS equations. The results of numerical experiments and data comparison are presented in Section 4. In Section 5 we give some final remarks.

2. Radial basis function approximation. Given $N + 2$ distinct points x_0, \dots, x_{N+1} in \mathbb{R}^d , and the corresponding function values $u(x_0), \dots, u(x_{N+1})$, the standard RBF interpolation problem is to find an interpolant of the form

$$s(x) = \sum_{j=0}^{N+1} \lambda_j \phi(\|x - x_j\|),$$

where $\|\cdot\|$ is the Euclidean norm, $\lambda_j \in \mathbb{R}$, for $j = 0, \dots, N + 1$, and ϕ is the real-valued inverse multiquadric function, defined by $\phi(r) = 1/\sqrt{c^2 r^2 + 1}$. The coefficients $\lambda_0, \dots, \lambda_{N+1}$ are determined by imposing the interpolation conditions $s(x_j) = u(x_j)$, $j = 0, \dots, N + 1$, which lead to a symmetric system of linear equations

$$(2.1) \quad A\lambda = u,$$

where

$$\begin{aligned} A_{ij} &= \phi(\|x_i - x_j\|), \quad i, j = 0, \dots, N + 1, \\ u &= [u(x_0), \dots, u(x_{N+1})]^T, \\ \lambda &= [\lambda_0, \dots, \lambda_{N+1}]^T. \end{aligned}$$

Micchelli [15] proved that the inverse multiquadric (IMQ) radial basis function is positive definite, so the coefficient matrix in (2.1) is invertible.

The Lagrangian form of RBF, based on cardinal basis functions, gives an alternative formulation which has the advantage of allowing easy evaluation of linear spatial differential operators [5]. In order to obtain the cardinal basis functions $\psi_j(x)$, $j = 0, \dots, N + 1$, with the property

$$\psi_j(x_i) = \begin{cases} 1, & \text{if } x_i = x_j, \\ 0, & \text{if } x_i \neq x_j, \end{cases}$$

we consider the linear system

$$A\Psi(x) = \bar{\phi}(x),$$

where $\Psi(x) = [\psi_0(x), \dots, \psi_{N+1}(x)]^T$, $\bar{\phi}(x) = [\phi(\|x - x_0\|), \dots, \phi(\|x - x_{N+1}\|)]^T$, and the coefficient matrix A is as above.

Therefore, the RBF interpolation can alternatively be written in Lagrange form as

$$s(x) = \sum_{j=0}^{N+1} \psi_j(x) u(x_j).$$

Moreover, for a linear operator \mathcal{L} , we have

$$(2.2) \quad \mathcal{L}s(x) = \sum_{j=0}^{N+1} \mathcal{L}\psi_j(x) u(x_j).$$

Then, for $i = 0, \dots, N+1$, the undetermined coefficient vectors

$$\mathcal{L}\Psi(x_i) = [\mathcal{L}\psi_0(x_i), \dots, \mathcal{L}\psi_{N+1}(x_i)]^T$$

are computed by solving the linear system

$$A\mathcal{L}\Psi(x_i) = \mathcal{L}\bar{\phi}_i,$$

where $\mathcal{L}\bar{\phi}_i$ denotes the evaluation at the point x_i of the column vector

$$\mathcal{L}\bar{\phi}(x) = [\mathcal{L}\phi(\|x - x_0\|), \dots, \mathcal{L}\phi(\|x - x_{N+1}\|)]^T.$$

3. RBF-based collocation methods.

3.1. The RBF collocation method in global mode (RBF-G). In the Lagrangian form of the global RBF interpolation method for a time-dependent problem, the solution $u(x, t)$ is approximated by

$$(3.1) \quad s_u(x, t) = \sum_{j=0}^{N+1} \psi_j(x) u_j(t),$$

where $u_j(t) \approx u(x_j, t)$, for $t > 0$, and $u_j(0) = u(x_j, 0)$. The centers of the RBFs used in equation (3.1) consist of the set $\mathcal{X} = X_\Omega \cup X_{\partial\Omega}$, where $X_\Omega = \{x_j \in \Omega, j = 1, \dots, N\}$, $X_{\partial\Omega} = \{x_j \in \partial\Omega, j = 0, N+1\}$. For simplicity, we let the set \mathcal{X} coincide with the set of collocation points.

Note that the zero boundary conditions at $\partial\Omega$ are satisfied if the approximation formula (3.1) is a linear combination of ψ_1, \dots, ψ_N , and takes the form

$$(3.2) \quad s_u(x, t) = \sum_{j=1}^N \psi_j(x) u_j(t).$$

If we write $u_t = w$, equations (1.1) can be rewritten as follows

$$(3.3) \quad \begin{aligned} iv_t + v_{xx} + vu &= 0, \\ w_t - u_{xx} + u - |v|^2 &= 0, \\ u_t - w &= 0, \end{aligned}$$

with initial conditions

$$u(x, 0) = u_0(x), \quad w(x, 0) = w_0(x), \quad v(x, 0) = v_0(x), \quad x \in \Omega.$$

Discretizing the spatial variable at the node points, and substituting (3.2) in the PDEs (3.3), leads to the system of ODEs

$$(3.4) \quad \begin{aligned} i v'_k(t) &= - \sum_{j=1}^N \frac{d^2 \psi_j}{dx^2}(x_k) v_j(t) - v_k(t) u_k(t), \\ w'_k(t) &= \sum_{j=1}^N \frac{d^2 \psi_j}{dx^2}(x_k) u_j(t) - u_k(t) + v_k(t) \overline{v_k(t)}, \\ u'_k(t) &= w_k(t), \quad k = 1, \dots, N, \end{aligned}$$

where $\overline{v(t)}$ is the complex conjugate of $v(t)$. The matrix form of (3.4) is

$$(3.5) \quad \begin{aligned} i V'(t) &= -\Psi_{xx} V(t) - V(t) * U(t), \\ W'(t) &= \Psi_{xx} U(t) - U(t) + V(t) * \overline{V(t)}, \\ U'(t) &= W(t), \end{aligned}$$

where $\Psi_{xx} = [\frac{d^2 \Psi}{dx^2}(x_1), \dots, \frac{d^2 \Psi}{dx^2}(x_N)]^T$, $V(t) = [v_1(t), \dots, v_N(t)]^T$, $W(t) = [w_1(t), \dots, w_N(t)]^T$, $U(t) = [u_1(t), \dots, u_N(t)]^T$. Note that the symbol “*” represents element-wise multiplication.

Now write $V(t) = V_r(t) + i V_i(t)$, where the r and i indices indicate the real part and imaginary part of complex vector, respectively. By using this notation, (3.5) can be written as

$$\begin{bmatrix} V'_r(t) \\ V'_i(t) \\ W'(t) \\ U'(t) \end{bmatrix} = \begin{bmatrix} 0 & -\Psi_{xx} & 0 & 0 \\ \Psi_{xx} & 0 & 0 & 0 \\ 0 & 0 & 0 & \Psi_{xx} - I \\ 0 & 0 & I & 0 \end{bmatrix} \begin{bmatrix} V_r(t) \\ V_i(t) \\ W(t) \\ U(t) \end{bmatrix} + \begin{bmatrix} -V_i(t) * U(t) \\ V_r(t) * U(t) \\ V_r(t) * V_r(t) + V_i(t) * V_i(t) \\ 0 \end{bmatrix}.$$

This system of ODE can be solved by standard ODE solvers such as the solvers `ode23` and `ode15s` in MATLAB. An alternative scheme for solving the system of ODE is to use the time stepping technique. We can use the forward Euler time-stepping method for approximating the time derivative. Let $\delta t = T/M$, and define $t^n = n \delta t$, $n = 0, \dots, M$. If we assume that U^n , V_r^n , V_i^n and W^n are approximations of $U(t^n)$, $V_r(t^n)$, $V_i(t^n)$ and $W(t^n)$, we get

$$\begin{aligned} \begin{bmatrix} V_r^{n+1} \\ V_i^{n+1} \\ W^{n+1} \\ U^{n+1} \end{bmatrix} &= \begin{bmatrix} I & -\delta t \Psi_{xx} & 0 & 0 \\ \delta t \Psi_{xx} & I & 0 & 0 \\ 0 & 0 & I & \delta t (\Psi_{xx} - I) \\ 0 & 0 & \delta t I & I \end{bmatrix} \begin{bmatrix} V_r^n \\ V_i^n \\ W^n \\ U^n \end{bmatrix} \\ &+ \delta t \begin{bmatrix} -V_i^n * U^n \\ V_r^n * U^n \\ V_r^n * V_r^n + V_i^n * V_i^n \\ 0 \end{bmatrix}, \end{aligned}$$

where I is the $N \times N$ identity matrix.

3.2. The RBF collocation method in finite difference mode (RBF-FD). The finite difference method consists of approximating the derivative of a function u at a given point based on a linear combination of the value of u at some surrounding node points. The FD formula approximates the action of the linear operator \mathcal{L} in $x = x_k$ ($1 \leq k \leq N$) as follows

$$\mathcal{L}u(x_k) \approx \sum_{j=1}^N \tilde{\omega}_{(k,j)} u(x_j),$$

where $\tilde{\omega}_{(k,\cdot)}$, $k = 1 \dots, N$, are called the FD weights at node points x_k . They are usually computed using polynomial interpolation [6].

In the RBF-FD approach, the weights of the FD formulas are obtained using the RBF interpolation technique. This method allows us to determine the derivative approximation for each node point in a local support region. Let the supporting region for each interior node x_k be identified by choosing M_k nodes that are defined as

$$\text{support}(x_k) = \{x_j \in \Omega \mid 0 \leq \|x_j - x_k\| \leq R\}, \quad k = 1, \dots, N,$$

where R is the size of the local support and M_k is the total number of interior and boundary nodes which lie in the supporting region of the node x_k .

To derive the RBF weights $\omega_{(k,\cdot)}$ for each node x_k , $k = 1 \dots, N$, we approximate the spatial linear operator \mathcal{L} using (2.2) in the supporting region of x_k , i.e.,

$$\mathcal{L}u(x_k) \approx \sum_{j=1}^{M_k} \omega_{(k,j)} u(x_j),$$

where $\omega_{(k,j)} = \mathcal{L}\psi_j(x_k)$.

Discretizing the spatial variable in the governing equations (3.3) and approximating the RBF weights for $\mathcal{L} = \frac{\partial}{\partial x^2}$ leads to a system of ODEs

$$\begin{aligned} (3.6) \quad v'_k(t) &= - \sum_{j=1}^{M_k} \omega_{(k,j)} v_j(t) - v_k(t) u_k(t), \\ w'_k(t) &= \sum_{j=1}^{M_k} \omega_{(k,j)} u_j(t) - u_k(t) + v_k(t) \overline{v_k(t)}, \\ u'_k(t) &= w_k(t), \quad k = 1, \dots, N. \end{aligned}$$

The system of ODEs (3.6) can be rewritten in matrix form

$$\begin{bmatrix} V'_r(t) \\ V'_i(t) \\ W'(t) \\ U'(t) \end{bmatrix} = \begin{bmatrix} 0 & -\tilde{\Phi}_{xx} & 0 & 0 \\ \tilde{\Phi}_{xx} & 0 & 0 & 0 \\ 0 & 0 & 0 & \tilde{\Phi}_{xx} - I \\ 0 & 0 & I & 0 \end{bmatrix} \begin{bmatrix} V_r(t) \\ V_i(t) \\ W(t) \\ U(t) \end{bmatrix} + \begin{bmatrix} -V_i(t) * U(t) \\ V_r(t) * U(t) \\ V_r(t) * V_r(t) + V_i(t) * V_i(t) \\ 0 \end{bmatrix},$$

where the sparse matrix $\tilde{\Phi}_{xx} = [\omega_{(1,\cdot)}^T, \dots, \omega_{(N,\cdot)}^T]^T$ contains the RBF weights. The sparsity of $\tilde{\Phi}_{xx}$ is dependent on the distribution of points and the size of the local support R . Figure 3.1 shows the sparsity pattern of $\tilde{\Phi}_{xx}$ for different sizes of the local support.

The resulting system of ODEs can be solved by using an available ODE solver such as MATLAB's ode23, or by a time stepping technique.

4. Numerical results. In this section, we present some numerical results to demonstrate the validity and effectiveness of the proposed methods. The accuracy is measured by the root mean square (RMS) error and by the L_∞ error

$$\begin{aligned} \text{RMS} &= \left[\frac{1}{N} \sum_{j=1}^N \left(u_{\text{exact}}(x_j, t) - u_{\text{app}}(x_j, t) \right)^2 \right]^{\frac{1}{2}}, \\ L_\infty &= \|u_{\text{exact}}(x, t) - u_{\text{app}}(x, t)\|_\infty = \max_{1 \leq j \leq N} |u_{\text{exact}}(x_j, t) - u_{\text{app}}(x_j, t)|. \end{aligned}$$

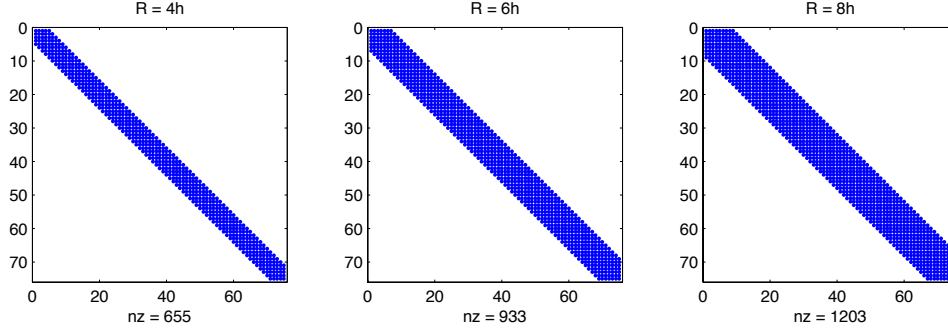


FIGURE 3.1. Sparsity pattern of matrix $\tilde{\Phi}_{xx}$ for equidistant points with different R .

The exact solution to equations (1.1) was derived in [13]:

$$\begin{aligned} v_r(x, t) &= 3\beta \operatorname{sech}^2(\beta x + \alpha t) \cos(\gamma x + (4\beta^2 - \gamma^2)t), \\ v_i(x, t) &= 3\beta \operatorname{sech}^2(\beta x + \alpha t) \sin(\gamma x + (4\beta^2 - \gamma^2)t), \\ u(x, t) &= 6\beta^2 \operatorname{sech}^2(\beta x + \alpha t), \quad x \in \Omega, t \geq 0, \end{aligned}$$

where $\alpha = \sqrt{4\beta^2 - 1}$, $\gamma = -\frac{\alpha}{2\beta}$, for $\beta \geq 1/2$. Numerical experiments are carried out with parameters $R = 6h$, $\beta = 1$, and $\Omega = [-10, 10]$. In our experiments, we use an equidistant points discretization $x_k = -10 + kh$, $0 \leq k \leq N + 1$, $h = 20/(N + 1)$, and Halton points discretization.

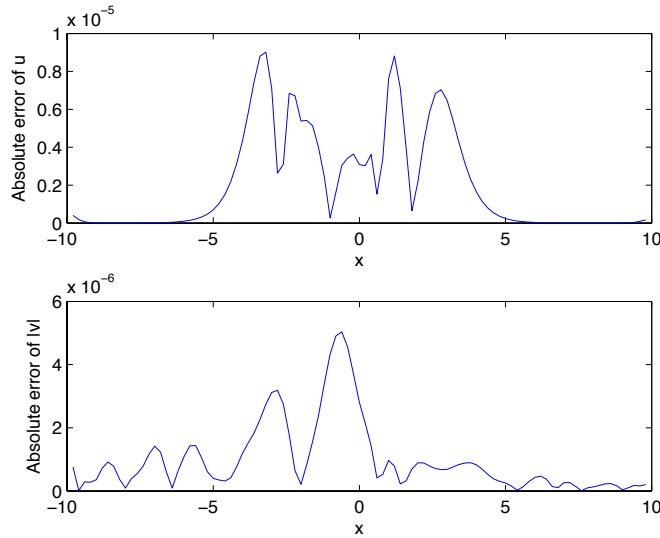


FIGURE 4.1. Absolute error of the RBF-FD method with $c = 0.5$ and $h = 0.2$, at $t = 1$.

Figures 4.1 and 4.2 show the absolute error of u and $|v|$, for the presented methods, at $t = 1$. If the shape parameter is chosen in a data-dependent way, i.e., if c is proportional of h ,

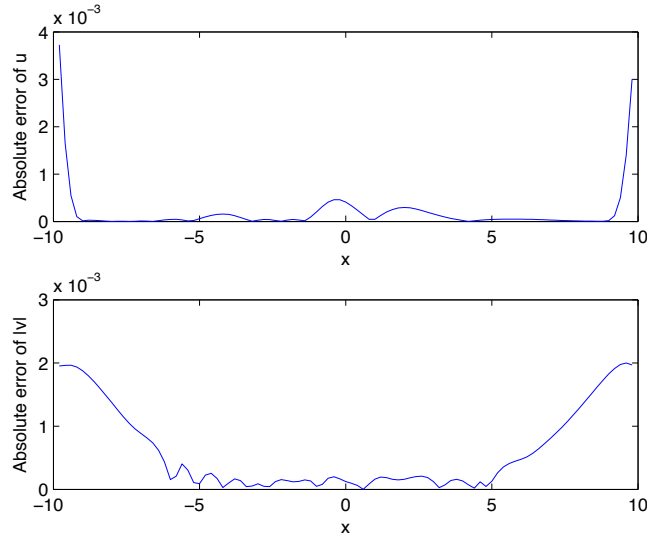


FIGURE 4.2. Absolute error of the RBF-G method with $c = 0.5$ and $h = 0.2$, at $t = 1$.

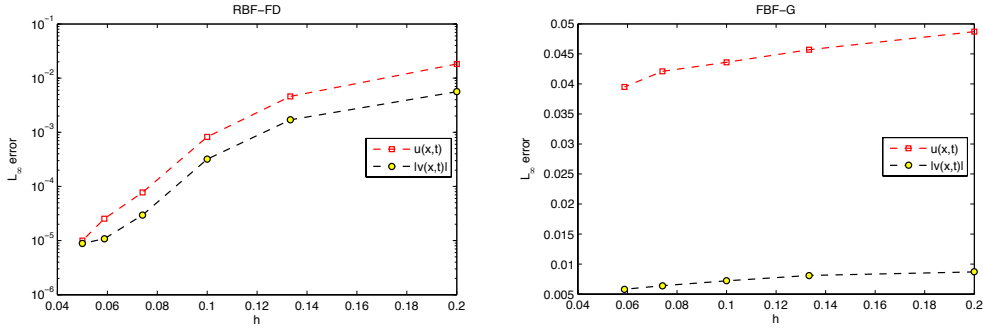


FIGURE 4.3. From left to right, the L_∞ error of the RBF-FD and RBF-G methods as a function of h , with $c = 1.5$, at $t = 1$.

the convergence rate cannot be shown, but this regime is of practical interest [3]. The RMS error and L_∞ error of the approximated solutions, for our proposed methods with equidistant points, are reported in Table 4.1. The numerical results of the Crank-Nicolson method with time-splitting spectral discretization (CN-TSSP) [2], for a time step 2×10^{-3} , are presented in the last column of Table 4.1. It can be seen that the numerical results obtained by the RBF-FD method are in good agreement with the exact solution, in contrast to the CN-TSSP method and the RBF-G method. Table 4.2 shows the accuracy of our proposed methods using the Halton distribution points. Note that in Table 4.1 and Table 4.2 we consider a data-dependent shape parameter. For a fixed shape parameter, the error goes to zero as the data points become denser. The error behavior and convergence rate are investigated for a fixed value of the shape parameter c [17] in Figure 4.3, where the error is displayed a function of h . For $c = 1.5$, the condition numbers of the coefficient matrices does not exceed 10^{10} when $0.05 \leq h \leq 0.2$.

Figure 4.4 displays the L_∞ error of the RBF-FD method and RBF-G method for different values of time. We can see that the error observed in the RBF-G method increases more than

TABLE 4.1

Error comparison of the approximated solutions for equidistant points with $h = 0.1$, $c = 0.9$, and $h = 0.2$, $c = 0.5$, at $t = 1$.

	h	RBF-G		RBF-FD		CN-TSSP	
		RMS	L_∞	RMS	L_∞	RMS	L_∞
$ v $	0.2	8.83e-4	2.00e-3	1.48e-6	5.04e-6	1.66e-5	4.77e-5
	0.1	6.61e-4	1.06e-3	1.06e-6	4.54e-6	1.50e-5	4.77e-5
u	0.2	5.48e-4	3.73e-3	3.32e-6	9.02e-6	2.65e-5	7.18e-5
	0.1	3.18e-4	2.19e-3	1.64e-6	7.74e-6	2.52e-5	7.18e-5

TABLE 4.2

Accuracy of the presented methods for 100 and 200 Halton points corresponding to $c = 0.5$ and $c = 1$, at $t = 1$.

	Number of points	RBF-G		RBF-FD	
		RMS	L_∞	RMS	L_∞
$ v $	100	1.25e-3	4.45e-3	3.77e-6	7.78e-6
	200	1.00e-3	4.30e-3	3.30e-6	7.37e-6
u	100	8.16e-4	4.85e-3	7.55e-6	3.96e-5
	200	6.97e-4	3.77e-3	6.98e-6	2.41e-5

when using the RBF-FD method. In Figure 4.5, the L_∞ errors are shown for a different size of the local support.

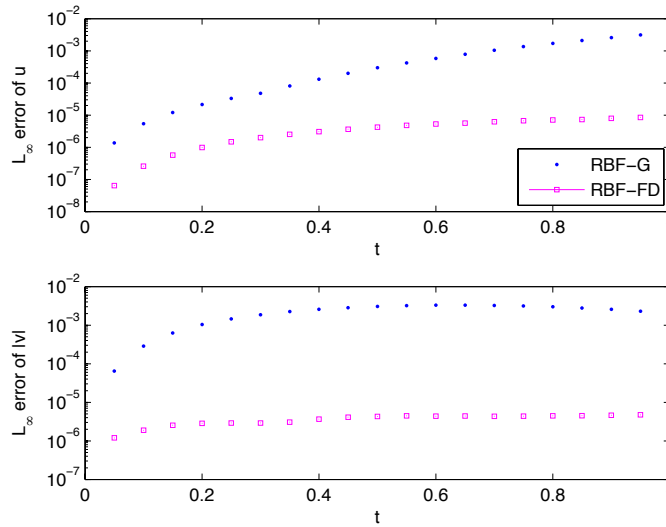


FIGURE 4.4. L_∞ error as a function of time for u and $|v|$, with $h = 0.2$ and $c = 0.5$.

5. Conclusion. In this paper, the collocation methods based on the RBF-G and RBF-FD methods for the coupled Klein-Gordon-Schrödinger equations are presented. It is shown that these methods require only a scattered set of nodes in the domain instead of a mesh, which is the case for traditional methods such as FEM or FDM. Experimental results show that the proposed methods for the numerical solution of the KGS equations are very accurate. Also,

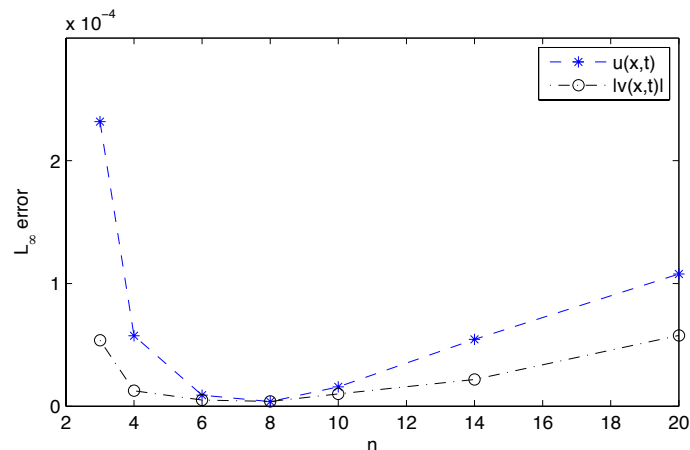


FIGURE 4.5. L_∞ error as a function of $R = nh$, with $h = 0.2$ and $c = 0.5$, at $t = 1$.

it is shown that the coefficient matrix of the RBF-FD method is sparse, and that this method has a good accuracy, as compared to the RBF-G and CN-TSSP methods.

Acknowledgement. The authors would like to thank E. Larsson and A. Heryudono for their helpful suggestions. As well, they acknowledge the useful remarks of the two referees, that greatly contributed to improve this paper.

REFERENCES

- [1] A. BACHELOT, *Probleme de Cauchy pour des systems hyperboliques semi-lineaires*, Ann. Inst. H. Poincaré Anal. Non Linéaire, 1 (1984), pp. 453–478.
- [2] W. BAO AND L. YANG, *Efficient and accurate numerical methods for the Klein-Gordon-Schrödinger equations*, J. Comput. Phys., 225 (2007), pp. 1863–1893.
- [3] J. P. BOYD, *Error saturation in Gaussian radial basis function on a finite interval*, J. Comput. Appl. Math., 234 (2010), pp. 1435–1441.
- [4] P. CHINCHAPATNAM, *Radial basis function based meshless methods for fluid flow problems*, Ph.D. thesis, School of Engineering Sciences, University of Southampton, 2006.
- [5] G. E. FASSHAUER, *Meshless methods*, in Handbook of Theoretical and Computational Nanotechnology, M. Rieth and W. Schommers, eds., American Scientific Publishers, 2005, pp. 24–26.
- [6] B. FORNBERG, *Calculation of weights in finite difference formulas*, SIAM Rev., 40 (1998), pp. 685–691.
- [7] C. FRANKE AND R. SCHABACK, *Solving partial differential equations by collocation using radial basis functions*, Appl. Math. Comput., 93 (1998), pp. 73–82.
- [8] I. FUKUDA AND M. TSUTSUMI, *On coupled Klein-Gordon-Schrödinger equations II*, J. Math. Anal. Appl., 66 (1978), pp. 358–378.
- [9] I. FUKUDA AND M. TSUTSUMI, *On coupled Klein-Gordon-Schrödinger equations III*, Math. Japon., 24 (1979), pp. 307–321.
- [10] A. GOLBABAI AND A. SAFDARI-VAIGHANI, *A meshless method for numerical solution of the coupled Schrödinger-KdV equations*, Computing, 92 (2011), pp. 225–242.
- [11] B. L. GUO AND C. X. MIAO, *Asymptotic behavior of coupled Klein-Gordon-Schrödinger equations*, Sci. China Ser. A., 25 (1995), pp. 705–714.
- [12] N. HAYASHI AND W. VON WAHL, *On the global strong solutions of coupled Klein-Gordon-Schrödinger equations*, J. Math. Soc. Japan, 39 (1987), pp. 489–497.
- [13] F. T. HIOE, *Periodic solitary waves for two coupled nonlinear Klein-Gordon and Schrödinger equations*, J. Phys. A, 36 (2003), pp. 7307–7330.
- [14] W. JIA, L. BIAO, AND Y. WANG-CHUAN, *Approximate solution for the Klein-Gordon-Schrödinger equation by the homotopy analysis method*, Chinese Phys. B, 19 (2010), 30401 (7 pages).
- [15] C. A. MICCHELLI, *Interpolation of scattered data: distance matrix and conditionally positive definite functions*, Const. Approx., 2 (1986), pp. 11–22.

- [16] H. POWER AND V. BARRACO, *A comparison analysis between unsymmetric and symmetric radial basis function collocation methods for the numerical solution of partial differential equations*, Comput. Math. Appl., 43 (2002), pp. 551–583.
- [17] R. SCHABACK AND H. WENDLAND, *Kernel techniques: From machine learning to meshless methods*, Acta Numer., 15 (2006), pp. 543–639.
- [18] C. SHU, H. DING, AND K. S. YEO, *Local radial basis function-based differential quadrature method and its application to solve two-dimensional incompressible Navier-Stokes equations*, Comput. Methods Appl. Mech. Engrg., 192 (2003), pp. 941–954.
- [19] M. L. WANG AND Y. B. ZHOU, *The periodic wave solutions for the Klein-Gordon-Schrödinger equations*, Phys. Lett. A., 318 (2003), pp. 84–92.
- [20] G. B. WRIGHT AND B. FORNBERG, *Scattered node compact finite difference-type formulas generated from radial basis functions*, J. Comput. Phys., 212 (2006), pp. 99–123.
- [21] X. M. XIANG, *Spectral method for solving the system of equations of Schrödinger-Klein-Gordon field*, J. Comput. Appl. Math., 21 (1988), pp. 161–171.
- [22] H. YUKAWA, *On the interaction of elementary particles I*, Proc. Phys. Math. Soc. Japan, 17 (1935), pp. 48–57.